Tuning the hydrophobicity of mica surfaces by hyperthermal Ar ion irradiation

Adrian Keller,[1,a)] Monika Fritzsche,[2] Ryosuke Ogaki,[1] Ilko Bald,[1] Stefan Facsko,[2] Mingdong Dong,[1] Peter Kingshott,[1] and Flemming Besenbacher[1,3]
[1]*Interdisciplinary Nanoscience Center (iNANO), Aarhus University, Ny Munkegade, 8000 Aarhus C, Denmark*
[2]*Institute of Ion Beam Physics and Materials Research, Helmholtz-Zentrum Dresden-Rossendorf, P.O. Box 510119, 01314 Dresden, Germany*
[3]*Department of Physics and Astronomy, Aarhus University, 8000 Aarhus C, Denmark*

(Received 29 November 2010; accepted 10 February 2011; published online 9 March 2011)

The hydrophobicity of surfaces has a strong influence on their interactions with biomolecules such as proteins. Therefore, for *in vitro* studies of bio-surface interactions model surfaces with tailored hydrophobicity are of utmost importance. Here, we present a method for tuning the hydrophobicity of atomically flat mica surfaces by hyperthermal Ar ion irradiation. Due to the sub-100 eV energies, only negligible roughening of the surface is observed at low ion fluences and also the chemical composition of the mica crystal remains almost undisturbed. However, the ion irradiation induces the preferential removal of the outermost layer of K^+ ions from the surface, leading to the exposure of the underlying aluminosilicate sheets which feature a large number of centers for C adsorption. The irradiated surface thus exhibits an enhanced chemical reactivity toward hydrocarbons, resulting in the adsorption of a thin hydrocarbon film from the environment. Aging these surfaces under ambient conditions leads to a continuous increase of their contact angle until a fully hydrophobic surface with a contact angle $>80^\circ$ is obtained after a period of about 3 months. This method thus enables the fabrication of ultrasmooth biological model surfaces with precisely tailored hydrophobicity. © *2011 American Institute of Physics*. [doi:10.1063/1.3561292]

I. INTRODUCTION

The presence of surfaces and interfaces influences many chemical and biological processes. Especially in the physiological environment, biological molecules such as proteins interact not only with a large variety of biological surfaces, including cell membranes, the surfaces of bones, and the walls of blood vessels, but also with nonbiological surfaces such as implants, dialysis membranes, and tubing. The proteins may adsorb to these surfaces which usually alters their conformation, both on the secondary and the tertiary structure levels.[1] In addition, the way of interaction is often dictated by the physicochemical properties of these sorbent surfaces, e.g., by their hydrophobicity, charge, chemical composition, or topography.

In order to understand the influence of the different surface properties on the bio-surface interaction, *in vitro* studies using model surfaces with tailored physicochemical properties are necessary. Especially the control of the hydrophobicity of the model surface is of particular interest, since the hydrophobicity determines the nature of the interactions between surface and protein, i.e., electrostatic versus hydrophobic interactions, and thus often has a tremendous effect on adsorption and aggregation.[2,3] However, the fabrication of model surfaces with tuned hydrophobicity so far remains challenging. In the past, different types of model surfaces, e.g., hydrophilic mica versus hydrophobic graphite[4] or different polymers,[3,5] have typically been compared, or chemical surface modifications such as silanization[2,6] were introduced. In addition to different chemical compositions, the fabricated model surfaces often exhibit a rather high surface roughness that can easily exceed several tens of nanometers and is typically very hard to control.[5,7] Therefore, it is difficult to separate the influence of the hydrophobicity on the bio-surface interactions from that of the surface roughness and the other chemical and physical properties of the model surfaces.[5]

In this paper, we present a method to precisely tune the hydrophobicity of mica surfaces by hyperthermal (<100 eV) ion bombardment without significant effect on the chemical composition or the surface topography. Muscovite mica is commonly used as a model surface for the study of biomolecules at the solid–liquid interface, especially by atomic force microscopy (AFM).[4,8] It has the ideal formula $KAl_2(Si_3AlO_{10})(OH)_2$ and, as can be seen in Fig. 1, consists of negatively charged aluminosilicate sheets that are electrostatically bound to alternating layers of K^+ ions. Due to its layered structure, mica can be easily cleaved which yields an atomically flat surface. Under aqueous conditions K^+ ions are exchanged into solution which results in an extremely hydrophilic surface with a negative net charge. Thus, mica has been used as a model surface to mimic cell membranes in several *in vitro* studies.

The response of mica crystals to heavy ion irradiation has been a subject of scientific interest for more than two decades.[9] Especially the formation of latent tracks and nanoscale hillocks induced by swift heavy[10,11] and slow highly charged ion impact,[12,13] respectively, received considerable attention. More recently, low energy ion

a)Electronic mail: adrian@inano.au.dk.

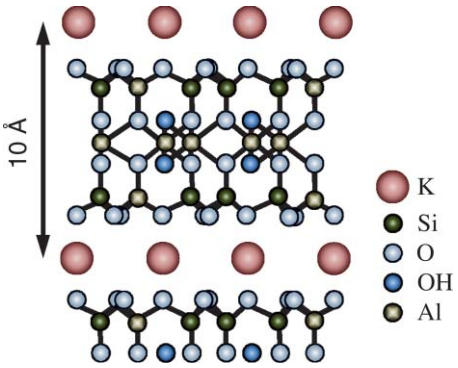

FIG. 1. Side view of the crystalline structure of muscovite mica.

bombardment[14,15] and plasma treatment[16] have been used to modify the properties of mica surfaces for various applications such as organic thin film growth.[15] During keV and sub-keV heavy ion bombardment, the well-defined layered structure of the crystalline mica surface is destroyed and its first few nanometers are amorphized due to the damage induced by the ion impact. Thus, the number of K^+ ions occupying surface sites is significantly reduced which in turn leads to a reduced charging of the surface in aqueous solution.[17] In addition, preferential sputtering may lead to an enrichment of Al or Si in the surface[17–19] which then results in an alteration of the chemical surface properties.[16,19] Furthermore, the ion bombardment may also induce a change of the surface topography.[17,18] These alterations are disadvantageous for the fabrication of biological model surfaces since the chemical[20] and topological[21] surface properties also affect the interaction of biomolecules with the surface.

As a more gentle technique for the surface treatment, we have utilized sub-100 eV Ar^+ ion bombardment to modify the physicochemical properties of the mica surface. At such hyperthermal energies, the energy and momentum transfer to the lattice atoms is too small to cause a significant atomic displacement so that the surface is expected to remain essentially crystalline[22] without any significant changes of the surface composition or topography. Nevertheless, after the irradiation, the contact angle of the mica surface is found to increase continuously with time until it reaches a stationary value $>80^\circ$ after a period of about 3 months. X-ray photoelectron spectroscopy (XPS) and AFM force spectroscopy indicate that this increase in hydrophobicity is caused by the increased adsorption of hydrocarbons (HCs) resulting from an enhanced chemical reactivity of the irradiated mica surface. This method thus offers the possibility of tailoring the contact angle of the ultrasmooth mica/HC surface for studying the detailed influence of hydrophobicity on bio-surface interactions[3,4] and for other applications such as evaporative deposition.[23]

II. EXPERIMENTAL

The Ar^+ ion irradiation was performed in a vacuum chamber with a base pressure of about 10^{-8} mbar. A standard Kaufman type ion source was used to bombard commercially available muscovite mica samples (grade V2 from Ted Pella, Inc.) which were cleaved directly before introduction into the vacuum. The irradiation was performed under normal incidence at room temperature and without additional electron flooding of the samples. The applied ion flux ranged from $\sim 2 \times 10^{12}$ to $\sim 2 \times 10^{14}$ $cm^{-2}s^{-1}$. After bombardment, the samples have been stored under ambient conditions in polystyrene sample boxes.

Recently-advanced contact angles of sessile drops of Milli-Q water have been measured using a drop shape analyzer DSA100 from Krüss GmbH and a circular fitting algorithm. Here, we report only contact angle values larger than 10° because smaller angles, e.g., for the freshly cleaved mica surface, could not be determined reliably from the fits. The values were averaged over four drops of different volume ranging from ~ 2 to ~ 50 μl placed at four different spots on the individual sample surfaces.

The surface topography has been analyzed by tapping mode AFM in air using a multimode scanning probe microscope with a NanoScope V controller from Veeco Instruments and PointProbe Plus tips for noncontact and tapping mode operation from NANOSENSORS. AFM force spectroscopy has been performed using a JPK NanoWizard II AFM and Olympus OMCL-TR400PSA cantilevers with Si_3N_4 tips and a nominal spring constant of 80 mN/m. In order to minimize deviations resulting from different tip radii, only force–distance curves are compared that have been taken with the same tip. The tip-sample distance D was calibrated by assigning a repulsive force of 100 pN to $D = 0$. The presented force–distance curves have been averaged over 20 individual approach curves taken at different positions on the sample surfaces.

The XPS data acquisition was performed using Kratos Axis UltraDLD instrument (Kratos Analytical Ltd.) equipped with a monochromated $Al_{K\alpha}$ x-ray source ($h\nu = 1486.6$ eV) operated at 15 kV and 15 mA (225 W). A hybrid lens mode (electrostatic and magnetic) was employed and three random areas were analyzed on each sample with the analysis area of 700 μm $\times$ 300 μm. The spectra were acquired at a photoemission angle of 90° with respect to the surface providing a probe depth of ~ 10 nm.[24] Survey spectra (binding energy (B.E.) of 0–1100 eV with pass energy of 160 eV) were used for element identification and quantification. High resolution (HR) spectra (with pass energy of 20 eV) of C 1s/K 2p region (B.E. of 278–298 eV) were obtained to determine the chemical state information. The acquired data were converted to VAMAS format and analyzed using CASAXPS software.

III. RESULTS AND DISCUSSION

Irradiation of the mica surface with noble gas ions of the energy of some hundred eV results both in a breakdown of the crystalline structure and, due to preferential sputtering, in a change of the chemical composition of the surface.[17] For ion energies well below 100 eV, however, no amorphisation is expected.[22] In addition, due to the low sputter yields,[25] preferential sputtering should result in only minor alterations of the chemical composition, especially at rather low fluences. Nevertheless, molecular dynamics simulations[26] and low-temperature (150 K) irradiation experiments[27] revealed that even at ion energies down to 10 eV a significant num-

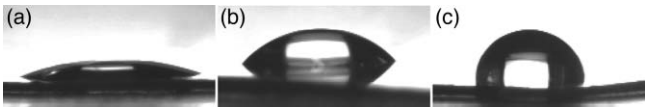

FIG. 2. Droplets of Milli-Q water on (a) an untreated mica surface and (b) and (c) a mica surface bombarded with 25 eV Ar ions at a fluence of 5×10^{14} cm^{-2}. The age of the samples is 10 (a), 7 (b), and 84 days (c).

ber of adatoms can be produced on the surface. However, in the case of the present room temperature irradiations at comparatively high ion fluxes and with a typical ion energy of 25 eV, we expect (i) a very low adatom yield, (ii) that a significant fraction of the surface damage is dynamically annealed during the irradiation, and (iii) that thermal surface diffusion heals at least some of the remaining damage in the hours and days following the irradiation.

It is therefore surprising that after irradiation with 25 eV Ar ions at fluences $\geqq 5 \times 10^{14}$ cm^{-2} the mica surfaces are found to be significantly more hydrophobic than the untreated ones as shown in Fig. 2. A freshly cleaved mica surface is extremely hydrophilic exhibiting a contact angle of less than 5°. When stored under ambient conditions, the contact angle of a cleaved mica surface is slowly increasing with time.[23] In our investigation, the contact angles of untreated mica surfaces never exceeded a value of 35° over a period of several months. In contrast, the ion bombarded surfaces exhibit considerably larger contact angles of $\gtrsim$40° already after aging for a few days [see Figs. 2(a) and 2(b)]. In addition, the contact angle is drastically increasing during further aging as can be seen in Figs. 2(b) and 2(c).

The time dependence of the contact angle θ of mica surfaces bombarded under different conditions as well as of untreated surfaces is depicted in Fig. 3(a). The contact angle of the irradiated surfaces is continuously increasing in the range from ~40° to more than 80°, resulting in a hydrophobic surface after a period of about 3 months. Interestingly, neither the ion energy nor the applied ion fluence has a pronounced effect on the surface hydrophobicity. The exponential fit (solid line in Fig. 3) yields a final value of the contact angle $\theta_0 \sim 84°$ and a time constant of $\tau \sim 29$ days. The contact angle of the virgin mica surface is found to increase as well but at a considerably lower rate.

It is well known that the surface topography can influence the wettability of a surface.[28] Therefore, AFM measurements have been performed in order to reveal possible alterations of the surface topography due to the irradiation. Although the ion bombarded surfaces remain rather flat, their root-mean-square (rms) surface roughness is found to increase from about 0.6 Å of the untreated mica surface to about 1.0 Å after irradiation. This increase of the surface roughness might result from the formation of adatom and surface vacancy islands as discussed above.[27] However, according to theoretical descriptions of surface wetting which have also been confirmed experimentally,[29,30] increasing the roughness of a hydrophilic surface such as the freshly cleaved mica surface in the current experiments makes the surface even more hydrophilic. In addition, previous experimental studies reported considerable variations of the contact angle (i.e.,

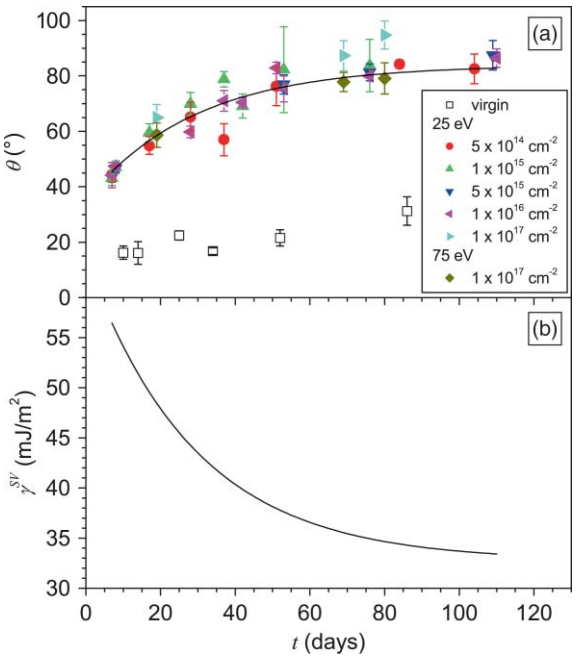

FIG. 3. (a) Time dependence of the contact angle θ of ion-irradiated and virgin mica surfaces. The solid line represents an exponential fit to the data of the bombarded samples. (b) Surface energy γ^{SV} as a function of aging time calculated from the fit in (a) following Ref. 33.

changes of the order of a few degrees) only for rms values exceeding 6 Å.[31,32] Therefore, we consider it unlikely that the observed strong increase of the contact angle is caused by the increased surface roughness and rather attribute it to changes in the surface energy of the irradiated mica surfaces. Thus, the surface energy γ^{SV} of the irradiated mica surfaces has been calculated as a function of time from the exponential fit in Fig. 3(a) by applying the equation-of-state approach proposed by Neumann *et al.*[33] As can be seen in Fig. 3(b) γ^{SV} decreases exponentially from 56.5 to 33.4 mJ/m^2. This decrease of the surface energy could, e.g., be caused by the adsorption of larger amounts of HCs on the ion bombarded compared to the untreated mica surfaces. In order to visualize a possible increased adsorption, the ion irradiation has been performed through a Cu grid so that only a fraction of the mica surface is modified. Figure 4(a) shows an AFM image of the resulting surface taken 12 days after the bombardment at the border between an irradiated (left) and a nonirradiated area (right). The corresponding height profile [Fig. 4(b)] reveals that the irradiated area is about 2.5 Å higher than the nonirradiated one. This indeed indicates an increased adsorption of HCs on the irradiated mica surface.

The crystalline mica surface is almost entirely chemically inert.[34] The amorphous mica surfaces created by keV and sub-keV ion bombardment exhibit more active surface sites and thus have an increased chemical activity which leads to a higher amount of adsorbed HCs,[19] a mechanism that can be neglected at the low energies used in the present experiments. On the other hand, it is known that sub-100 eV noble gas ion irradiation may create dangling bonds on the irradiated surface, an effect that plays an important role in the plasma-assisted growth of HC films.[35] Thus, one could assume that

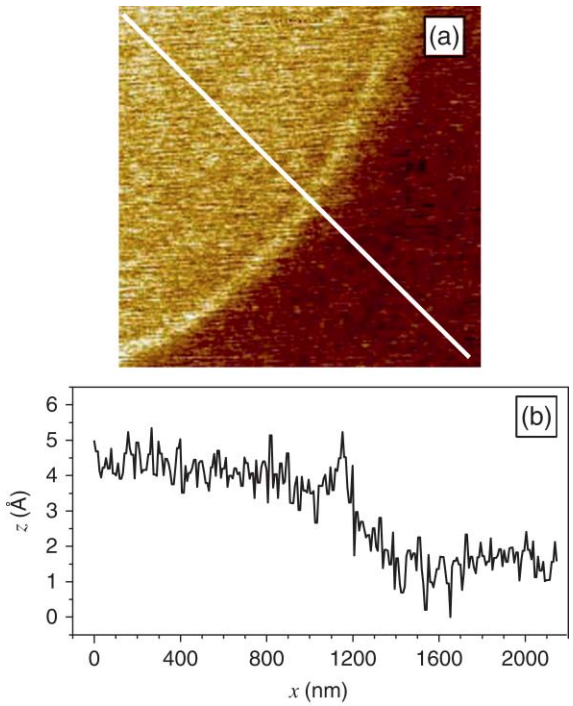

FIG. 4. (a) AFM image of a mica surface bombarded with 50 eV Ar^+ through a grid. The applied fluence was 5×10^{15} cm^{-2} and the sample has been aged for 12 days. The size of the image is 1.57×1.57 μm^2. (b) Corresponding height profile along the white line in (a).

the mica surface exhibits dangling bonds after the irradiation which are saturated by bonding to HCs from the environment when the sample is extracted from the vacuum and exposed to the laboratory atmosphere. This increased adsorption would lead to a more hydrophobic surface. In this case, the mica surface should become hydrophilic again after removing the HC film and then show a similar time dependence of the contact angle as the untreated surface.

Therefore, an untreated mica surface ($\theta = 15^\circ$) and an irradiated mica surface ($\theta = 87^\circ$) have been UV/ozone exposed for one hour which should oxidize and thus remove all adsorbed HCs. Indeed, after the treatment, both surfaces are hydrophilic again and show contact angles smaller than 5° just as a freshly cleaved surface. This confirms the above assumption that the increased hydrophobicity is caused by HC adsorption. However, after the UV/ozone treatment, the contact angle of the bombarded mica surface is again found to increase much faster than the one of the untreated surface and finally reaches the saturation value it had before the UV/ozone cleaning (see Fig. 5). This observation is at variance with the above interpretation that the increased HC adsorption results from the creation of dangling bonds during the bombardment since all dangling bonds should be saturated after the ozone treatment. The observed rapid increase after the cleaning rather indicates that the higher HC adsorption results from a permanent alteration of the chemical composition of the surface due to the irradiation.

In order to investigate the influence of the ion irradiation on the chemical composition of the mica surfaces, the atomic concentrations in atomic percent (at.%) of the main components of three differently treated mica samples after aging for

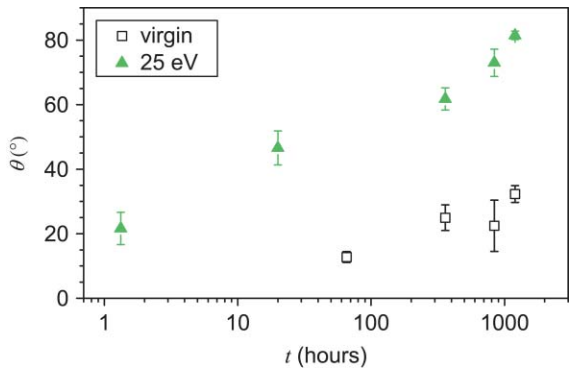

FIG. 5. Time dependence of the contact angle θ of ion-irradiated and virgin mica surfaces after ozone/UV cleaning for 1 h.

4 days have been determined from XPS measurements. The results are given in Fig. 6. The determined atomic concentrations of the virgin sample are in fair agreement with the theoretical values for an ideal muscovite mica crystal although a slightly higher K concentration is observed. Furthermore, ~5 at.% of C are found on the aged mica surface, resulting from adsorbed HCs. After irradiation with 10^{15} and 10^{16} Ar ions/cm^2, considerably increased C concentrations of ~10 at.% and ~27 at.%, respectively, are found. An inverse trend is observed for the K concentration which is reduced after the irradiations. The concentrations of O, Si, and Al on the other hand remain almost unaffected in the low-fluence case whereas an enrichment of Al accompanied by a depletion of O and Si is found after the high-fluence irradiation.

Although a similar Al enrichment has been observed for higher ion energies and attributed to preferential sputtering,[17] this effect should be very small for 25 eV ion energy which is close to or even smaller than the sputtering threshold energy (typically 5–40 eV).[25] However, also a significant fraction (up to 16%)[36] of doubly charged Ar ions is extracted from the plasma of the Kaufman ion source. The observed change in surface composition can thus to a large extent be attributed to preferential sputtering due to the impact of 50 eV Ar^{2+} ions.

Nevertheless, the altered O, Si, and Al concentrations are not the origin of the enhanced HC adsorption since an increased C content is already found at the lower fluence

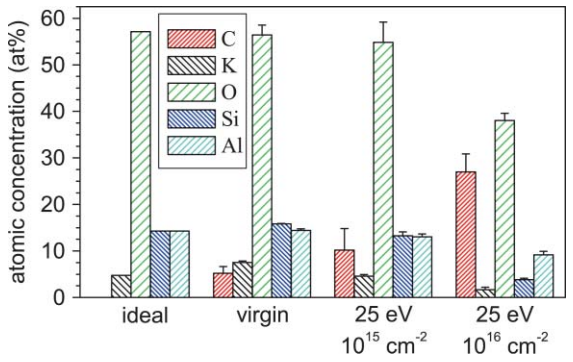

FIG. 6. Atomic concentrations in atomic percent (at.%) determined from survey-scan XP spectra of an untreated and two 25 eV-irradiated mica surfaces of different fluences after 4 days of aging. For comparison, also the theoretical concentrations for an ideal mica crystal are given.

TABLE I. Elemental concentrations of K and C (in at.%) of virgin and irradiated mica surfaces aged for different times.

	Virgin			25 eV, 10^{15} cm^{-2}	
Element	10 min	4 days	64 days	4 days	67 days
K	7.3 ± 0.1	7.6 ± 0.3	6.1 ± 1.6	4.6 ± 0.4	2.2 ± 0.3
C	6.1 ± 0.1	5.2 ± 1.4	10.5 ± 3.7	10.2 ± 4.6	18.4 ± 0.6

of 10^{15} cm^{-2} (see Fig. 6). On the other hand, for both low and high fluences a reduced K concentration is observed. It has been shown previously that a K depletion may increase the chemical activity of the mica surface because the silicate tetrahedra of the surface are the main centers for C adsorption.[37] Therefore, when the outermost layer of K ions is removed from the surface due to the irradiation, the first aluminosilicate sheet is exposed and HCs from the environment can bind to the active silicate centers. The removal of the K^+ ions from the surface by the impact of hyperthermal heavy ions seems to be very efficient even at the lowest fluence applied. This high efficiency probably results from the fact that the K^+ ions are not covalently but electrostatically bound to the negatively charged aluminosilicate sheets so that the implantation of the Ar^+ ions between these two layers induces the desorption of K due to electrostatic repulsion similar to a Coulomb explosion.[38]

In order to study the increase of hydrophobicity with time, further XPS measurements have been performed on irradiated and virgin samples of different age. The K and C concentrations for virgin and irradiated mica after different periods of aging are given in Table I. It is interesting to note that the C content of a virgin mica sample does not change significantly between 10 min and 4 days of aging which implies that all the available adsorption sites get rapidly occupied by HCs either from the laboratory atmosphere or from the residual gas in the vacuum chamber. For longer aging, however, it is found that for both virgin and irradiated mica the K concentration slowly decreases with age. This depletion of K is caused by the fact that under ambient conditions every surface is covered by a thin film of water. Then, similar to the situation in liquid, K ions are exchanged into solution. As a consequence of the K depletion, the amount of adsorbed HCs increases slowly (see Table I).

This interpretation is further supported by Fig. 7 in which the C concentration is plotted as a function of the K concentration for various differently treated mica samples of different ages. A clear correlation between the K and the C concentrations is observed for all samples. Figure 7 furthermore reveals that the applied ion fluence has a stronger influence on the K and the C concentrations than the aging of the samples. The C concentration of the samples irradiated with the lower fluence is increasing considerably with the age of the samples whereas the C concentrations of the higher fluence samples show only a rather weak dependence on the aging time. This can again be explained with the strong K depletion after the high-fluence irradiation which means that the outermost K layer has almost completely been removed and only very few K^+ ions remain on the surface and block

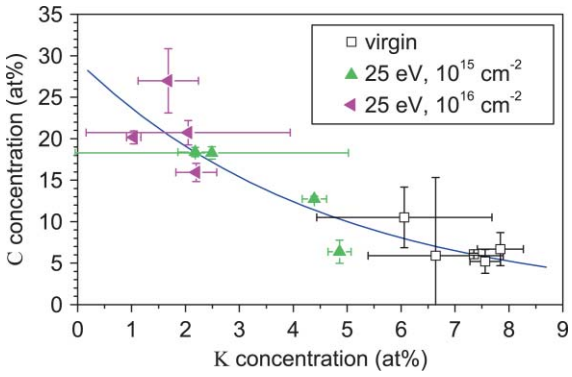

FIG. 7. Carbon concentration vs potassium concentration of various untreated and 25 eV-irradiated samples with ages ranging from 10 min to 166 days (virgin), from 4 to 169 days (10^{15} cm^{-2}), and from 4 to 194 days (10^{16} cm^{-2}). The solid line represents an exponential fit to the whole data set.

potential adsorption sites. Since, on the contrary, the contact angles of all the irradiated samples show a strong dependence on the aging but not on the ion fluence (cf. Fig. 3), it seems unlikely that the increase of hydrophobicity is solely caused by the different amounts of adsorbed HCs.

Carbon adsorbates on cleaved mica surfaces are known to consist mainly of saturated HCs but also include small fractions of oxidized HCs.[19] In the case of mica surfaces exposed to an Ar plasma, an increase of the fraction of oxygen-containing HCs has been observed.[19] Such an alteration of the fractions of adsorbed HC species could also affect the hydrophobicity of the surface. Therefore, high-resolution XP spectra of the C 1s and the K 2p peaks of virgin and irradiated mica samples after aging for different times have been taken and are displayed in Fig. 8. Since we do not expect any significant shift of the K 2p peaks due to aging or irradiation, the HR spectra in Fig. 8 have been calibrated using the K 2p peak positions.

The high-energy shoulders of the C 1s peaks in Fig. 8 can be attributed to the presence of carbon adsorbates with different functional groups. Curve fitting of the C 1s peaks using Gaussian distributions revealed chemical shifts in the

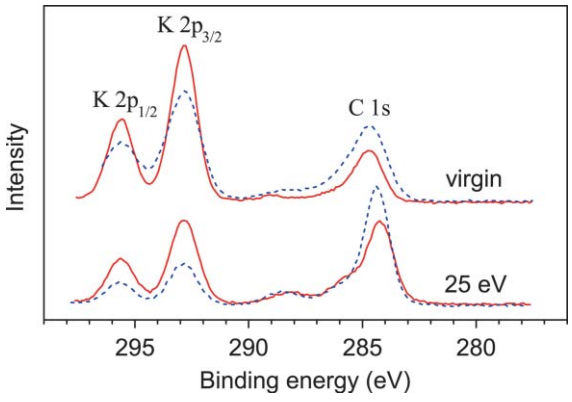

FIG. 8. High-resolution XP spectra showing the carbon C 1s and the potassium K 2p peaks of virgin and irradiated mica after different aging periods. The samples were aged for 4 days (solid lines) and 64 and 67 days for the virgin and the irradiated sample, respectively (broken lines). The applied ion fluence was 10^{15} cm^{-2}.

TABLE II. Peak positions (in eV) and peak area ratios (in %) of the functional groups contributing to the C 1s peaks for virgin and irradiated mica surfaces aged for different times. The applied ion fluence was 10^{15} cm^{-2}.

	C–C/C–H		C–OH		–COOH	
Sample, age	Position	Area ratio	Position	Area ratio	Position	Area ratio
Virgin, 10 min	284.7	72	286.2	19	289.1	9
Virgin, 4 days	284.7	72	286.3	18	288.9	10
Virgin, 64 days	284.7	69	286.4	20	288.6	11
25 eV, 4 days	284.2	68	285.8	20	288.1	12
25 eV, 67 days	284.4	72	285.9	17	288.5	11

range from +1.5 to +1.7 eV and from +3.9 to +4.4 eV (with respect to the C 1s peaks at 284.2 to 284.7 eV), corresponding to C–OH and COOH contributions, respectively.[39] The individual peak positions and the peak area ratios of the identified species for the different samples as obtained from the Gaussian fits are summarized in Table II. For all the samples, irradiated as well as untreated, rather large contributions from oxygen-containing HCs are observed with only minor differences in the HC fractions which we attribute to statistical fluctuations. These fluctuations might be related to the fact that on some of the samples investigated by XPS low concentrations of N (<3 at.%) have been found. Thus, also amine or amide groups might contribute to the observed chemical shifts of the C 1s peak. Nevertheless, the XPS measurements show that the chemical composition of the HC films is affected neither by the irradiation nor by the aging of the samples. Thus, the increase in hydrophobicity must have a different origin.

The wetting behavior of a surface is also sensitive to its charging in aqueous solution with polar surfaces typically being more hydrophilic. Due to the exchange of K^+ ions into solution, the mica surface exhibits a negative charge at all *p*H values. In order to determine possible variations in the charging of the modified mica surfaces, AFM force spectroscopy measurements have been performed in 3 mM KCl solution. Figure 9(a) gives the force–distance curve obtained for a freshly cleaved mica surface. For tip-sample distances $D \gtrsim 5$ nm, electrostatic repulsion between the negatively charged mica surface and the neutral Si_3N_4 tip causes a deflection of the cantilever.[40] At short distances $D < 5$ nm, the van der Waals attraction eventually overcomes the electrostatic repulsion and the tip snaps toward the surface ("snap-to-contact") causing a negative deflection of the cantilever. Any further approach results again in an increase of the repulsive force due to the Pauli exclusion. As can be seen from the force–distance curves given in Figs. 9(b) and 9(c), aging of the virgin mica surface leads to an increase in both the attractive and the repulsive forces at short and long distances, respectively. The stronger van der Waals forces indicate a change in the chemical nature of the surface which can be attributed to the presence of the adsorbed HC film whereas the stronger electrostatic repulsion results from the K depletion. In the case of the irradiated mica surfaces [Figs. 9(d) and 9(e)], an even stronger increase in the attractive forces at short distances are observed which can be interpreted as resulting from the higher amount of adsorbed HCs. However, in contrast to the nonirradiated mica surfaces, the repulsive electrostatic interactions at long distances become weaker with aging.

The electrostatic repulsive force F_e at distances larger than the Debye length λ_D of the electrolyte can be approximated as[40]

$$F_e \approx \frac{4\pi R}{\epsilon_0 \epsilon_w} \sigma_t \sigma_s \lambda_D e^{-D/\lambda_D} \tag{1}$$

with the dielectric constants ϵ_0 and ϵ_w of vacuum and water, respectively, and the tip radius R. σ_t and σ_s are the charge densities of the tip and the surface, respectively. The broken lines in Fig. 9 therefore represent fits to the force–distance

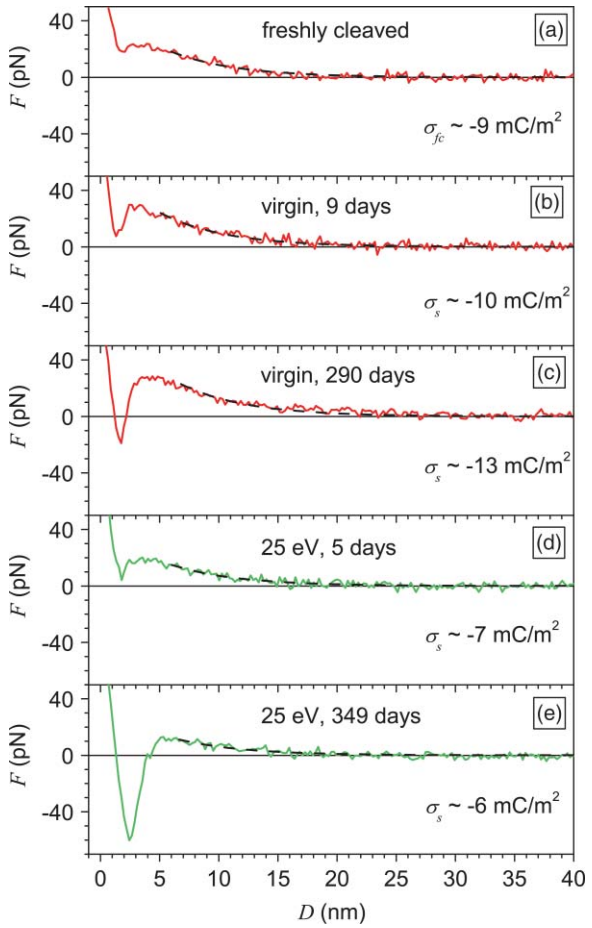

FIG. 9. Force–distance curves for (a–c) virgin and (d–e) irradiated mica surfaces of different age. The applied ion fluence was 5×10^{14} cm^{-2}. The broken lines represent exponential fits according to Eq. (2).

curves in the $D > 5$ nm region that follow the function

$$F = A\lambda_D e^{-D/\lambda_D}, \quad (2)$$

where A is the fitting parameter and $\lambda_D = 5.55$ nm for the 3 mM KCl solution.[40] Since the same tip was used for the aged and the freshly cleaved samples, the surface charge densities σ_s can be determined from the ratios of the fitting parameters, $\sigma_s/\sigma_{fc} = A/A_{fc}$, and the charge density of the freshly cleaved mica surface which, under the current buffer conditions, has a value of $\sigma_{fc} \sim -9$ mC/m^2.[40] The resulting charge densities are given together with the corresponding force–distance curves in Fig. 9. Interestingly, for prolonged aging, σ_s of the untreated mica samples increases by almost 50% [see. Fig. 9(c)] whereas the charge density of the irradiated mica surfaces is decreasing with age [Figs. 9(d) and 9(e)]. However, even after aging for almost one year, the irradiated mica surface still exhibits a significant charge of about $2/3\sigma_{fs}$.

At first glance, these results seem to contradict the above XPS measurements which revealed a lower K concentration on the irradiated mica surfaces. One would thus expect that the irradiated samples actually exhibit a higher surface charge than the virgin ones. This discrepancy can be explained by the adsorbed HC film, which has a larger thickness and acts as a dielectric that actually screens the increased charge density of the interface. This interpretation also offers an explanation for the increase of the hydrophobicity with time: removal of K ions from the mica surface either by aging or irradiation leads to the charging of the surface. The resulting surface is thus more hydrophilic. At the same time, however, a stronger K depletion leads to a larger amount of adsorbed HCs. A larger thickness of the HC film on the other hand leads to a stronger screening of the interface charge which in combination with the hydrophobic nature of the adsorbed HCs *effectively reduces* the hydrophilicity of the mica surface. In addition to the film thickness, the screening efficiency (i.e., the dielectric constant of the HC film) probably also depends on the conformation and the packing of the adsorbed HCs which may in turn depend again on the sample age and the irradiation conditions. The complex interplay between the different time and treatment dependencies of the individual mechanisms involved thus leads to the over-all behavior of the resulting hydrophobicity depicted in Fig. 3.

IV. CONCLUSION

In summary, we have introduced hyperthermal Ar^+ ion irradiation as a gentle technique to tune the physicochemical properties of mica surfaces and enhance their chemical reactivity. Due to the ultralow energies of the ions, only negligible roughening of the surface is observed and also the chemical composition remains almost undisturbed. Only at rather high fluences, preferential sputtering leads to the depletion of oxygen and silicon. Nevertheless, the preferential removal of K is observed already at significantly lower fluences which probably results from the repulsion between the implanted Ar^+ and the electrostatically bound K^+ ions that are located on surface sites. Due to the removal of the outermost K layer the underlying aluminosilicate sheets get exposed which feature a large number of centers for C adsorption. The resulting surface thus exhibits an enhanced reactivity and adsorbs large amounts of HCs from the environment.

Aging the irradiated samples under ambient conditions results in a continuous increase of the contact angle of the initially hydrophilic surface. After a period of about 3 months, the mica surface becomes fully hydrophobic with a contact angle of $> 80°$. Neither the applied ion fluence nor the ion energy (in the sub-100 eV range) has an influence on the hydrophobicity. The enhanced hydrophobicity of the irradiated samples is attributed to the interplay between the charging of the mica surface due to the K depletion and the increased adsorption of hydrophobic HCs which screen the charge. Due to the different age and treatment dependencies of the interface charge and the screening efficiency of the HC film, no simple correlation between the amount or chemical composition of the HC adsorbates and the hydrophobicity could be established. Nevertheless, we have demonstrated that hyperthermal ion irradiation is a versatile tool not only for the enhancement of the chemical reactivity of mica but also for the fabrication of ultrasmooth model surfaces with tailored hydrophobicity that do not exhibit significant chemical or topological modifications.

ACKNOWLEDGMENTS

We thank W. Kudernatsch and R. Bechstein for discussions and A. von Keudell for helpful comments. We would like to acknowledge financial support from the Danish Research Councils to the iNANO center, from the Carlsberg Foundation, from ERC for an advanced grant (F.B.) and from the Alexander von Humboldt foundation (A.K.).

[1] J. J. Gray, Curr. Opin. Struct. Biol. **14**, 110 (2004).
[2] M. van der Veen, M. C. Stuart, and W. Norde, Colloids Surf., B **54**, 136 (2007).
[3] C. Jeworrek, O. Hollmann, R. Steitz, R. Winter, and C. Czeslik, Biophys. J. **96**, 1115 (2009).
[4] W. Hoyer, D. Cherny, V. Subramaniam, and T. M. Jovin, J. Mol. Biol. **340**, 127 (2004).
[5] A. Nayak, A. K. Dutta, and G. Belfort, Biochem. Biophys. Res. Commun. **369**, 303 (2008).
[6] C. Pinholt, M. Fanø, C. Wiberg, S. Hostrup, J. T. Bukrinsky, S. Frokjaer, W. Norde, and L. Jorgensen, Eur. J. Pharm. Sci. **40**, 273 (2010).
[7] H. Zhuang, B. Song, V. V. S. S. Srikanth, X. Jiang, and H. Schönherr, J. Phys. Chem. C **114**, 20207 (2010).
[8] C. Goldsbury, J. Kistler, U. Aebi, T. Arvinte, and G. J. S. Cooper, J. Mol. Biol. **285**, 33 (1999).
[9] E. Dartyge and P. Sigmund, Phys. Rev. B **32**, 5429 (1985).
[10] F. Thibaudau, J. Cousty, E. Balanzat, and S. Bouffard, Phys. Rev. Lett. **67**, 1582 (1991).
[11] T. Hagen, S. Grafström, J. Ackermann, R. Neumann, C. Trautmann, J. Vetter, and N. Angert, J. Vac. Sci. Technol. B **12**, 1555 (1994).
[12] D. Schneider, M. A. Briere, M. W. Clark, J. McDonald, J. Biersack, and W. Siekhaus, Surf. Sci. **294**, 403 (1993).
[13] R. Ritter, G. Kowarik, W. Meissl, A. S. El-Said, L. Maunoury, H. Lebius, C. Dufour, M. Toulemonde, and F. Aumayr, Vacuum **84**, 1062 (2010).
[14] R. Buzio, A. Bosca, S. Krol, D. Marchetto, S. Valeri, and U. Valbusa, Langmuir **23**, 9293 (2007).
[15] G. Hlawacek, P. Puschnig, P. Frank, A. Winkler, C. Ambrosch-Draxl, and C. Teichert, Science **321**, 108 (2008).
[16] B. Liberelle, X. Banquy, and S. Giasson, Langmuir **24**, 3280 (2008).
[17] R. Buzio, A. Toma, A. Chincarini, F. Buatier de Mongeot, C. Boragno, and U. Valbusa, Surf. Sci. **601**, 2735 (2007).
[18] N. M. D. Brown and Z.-H. Liu, Appl. Surf. Sci. **90**, 155 (1995).

[19]Z. H. Liu and N. M. D. Brown, J. Phys. D: Appl. Phys. **31**, 1771 (1998).
[20]L. Treuel, M. Malissek, J. S. Gebauer, and R. Zellner, ChemPhysChem **11**, 3093 (2010).
[21]M. S. Lord, M. Foss, and F. Besenbacher, Nanotoday **5**, 66 (2010).
[22]H. Gnaser, *Low Energy Ion Irradiation of Solid Surfaces*, 1st ed. (Springer-Verlag, New York, 1998).
[23]K. F. Baughman, R. M. Maier, T. A. Norris, B. M. Beam, A. Mudalige, J. E. Pemberton, and J. E. Curry, Langmuir **26**, 7293 (2010).
[24]D. Briggs and J. T. Grant, *Surface Analysis by Auger and X-ray Photoelectron Spectroscopy* (IM Publications, Chichester, 2003).
[25]J. B. Malherbe, Crit. Rev. Solid State Mater. Sci. **19**, 55 (1994).
[26]H. Metiu and A. E. DePristo, J. Chem. Phys. **91**, 2735 (1989).
[27]T. Michely and C. Teichert, Phys. Rev. B **50**, 11156 (1994).
[28]J. Bico, U. Thiele, and D. Quéré, Colloids Surf., A **206**, 41 (2002).
[29]Z. Burton and B. Bhushan, Nano Lett. **5**, 1607 (2005).
[30]E. Martines, K. Seunarine, H. Morgan, N. Gadegaard, C. D.W. Wilkinson, and M. O. Riehle, Nano Lett. **5**, 2097 (2005).
[31]S. K. Rawal, A. K. Chawla, V. Chawla, R. Jayaganthan, and R. Chandra, Mat. Sci. Eng., B **172**, 259 (2010).
[32]S. Veeramasuneni, J. Drelich, J. Miller, and G. Yamauchi, Prog. Org. Coat. **31**, 265 (1997).
[33]A. W. Neumann, R. J. Good, C. J. Hope, and M. Sejpal, J. Colloid Interface Sci. **49**, 291 (1974).
[34]C. R. Kessel and S. Granick, Langmuir **7**, 532 (1991).
[35]C. Hopf, W. Jacob, and A. von Keudell, J. Appl. Phys. **97**, 094904 (2005).
[36]M. Zeuner, J. Meichsner, H. Neumann, F. Scholze, and F. Bigl, J. Appl. Phys. **88**, 611 (1996).
[37]K. G. Bhattacharyya, Langmuir **5**, 1155 (1989).
[38]H.-P. Cheng and J. D. Gillaspy, Phys. Rev. B **55**, 2628 (1997).
[39]S. Yumitori, J. Mater. Sci. **35**, 139 (2000).
[40]H.-J. Butt, Biophys. J. **60**, 1438 (1991).